

Synthesis, Spectroscopic Characterization, and Electro-Optical Properties of Noncentrosymmetric Azobenzene/Zirconium Phosphonate Multilayer Films

Dennis G. Hanken, Roberta R. Naujok, Jesse M. Gray, and Robert M. Corn*

Department of Chemistry, University of Wisconsin—Madison, 1101 University Avenue, Madison, Wisconsin 53706

Ultrathin noncentrosymmetric nonlinear optical films based on zirconium phosphonate (ZP) self-assembled multilayers that incorporate the asymmetric azobenzene chromophore [5-[4-[[4-[(6-hydroxyhexyl)sulfonyl]phenyl]-azo]phenyl]pentoxy]phosphonic acid (HAPA) are synthesized and constructed. The ZP film structure and multilayer deposition chemistry are characterized by a combination of polarization/modulation Fourier transform infrared reflection absorption spectroscopy, surface plasmon resonance (SPR) measurements, and optical second harmonic generation (SHG). SPR measurements on the HAPA multilayer films yield an average monolayer thickness of 27 ± 0.5 Å. The resonant SHG at 365 nm from ultrathin HAPA ZP films on silica surfaces increases quadratically with the number of self-assembled HAPA monolayers, and an analysis of the polarization dependence of the surface SHG yields an orientation parameter $D = 0.79 \pm 0.03$ corresponding to an average tilt angle of $27 \pm 2^\circ$ for the azobenzene chromophores with respect to the surface normal. An electro-optic coefficient r_{33} for the HAPA monolayers of 11 pm/V at 632.8 nm is obtained from SPR modulation experiments of ZP films on gold substrates that have been incorporated into air-gap capacitors. SPR modulation experiments are then performed on a HAPA monolayer in an in situ electrochemical environment in order to determine that a modulation of ± 25 mV corresponds to a change in the electric field strength of 1×10^4 V/cm within the ultrathin organic film at the electrode surface.

A wide variety of novel organic materials have been designed and synthesized for use in nonlinear optics.^{1–3} One important application of these nonlinear optical (NLO) materials is the creation of noncentrosymmetric thin organic films for electro-optical devices.^{4–6} The electro-optical or Pockel's effect results from a change in the index of refraction of a material upon application of an external electric field; this response requires a

noncentrosymmetric material and is described by the electro-optic coefficient, r .⁷ Current electro-optical devices are typically based on the inorganic crystal lithium niobate, LiNbO₃, which has an electro-optic coefficient, r_{33} , of 31 pm/V.⁸ Most of the research on molecular alternatives to LiNbO₃ have focused on the incorporation of NLO organic chromophores into polymer networks. These NLO polymers are poled in a strong electric field at elevated temperatures in order to create a noncentrosymmetric film. The electro-optic coefficients generated by such films vary from 1 to 55 pm/V in the presence of the poling fields but can decay significantly with time.^{9–14}

An alternative to poled polymer films are ultrathin noncentrosymmetric organic films that have been created one monolayer at a time with a self-assembly process. Marks et al. have shown that noncentrosymmetric NLO films of bifunctional stilbazole chromophores can be formed by covalent coupling reactions utilizing an organosilane-based chemistry.^{15–17} A second method for creating noncentrosymmetric self-assembled multilayers uses a zirconium phosphonate (ZP) ligand coupling chemistry first reported by Mallouk and co-workers for centrosymmetric films^{18–20} and subsequently modified by Katz et al. to create noncentrosymmetric multilayers.^{21–24} Ultrathin noncentrosymmetric films formed from ZP multilayers with NLO chromophores are more chemically and thermally stable than most NLO polymer films,²² but spec-

- (7) Shen, Y. R. *The Principles of Nonlinear Optics*; Wiley: New York, 1984.
- (8) Yariv, A.; Yeh, P. *Optical Waves in Crystals*; Wiley: New York, 1984.
- (9) Ahlheim, M.; Barzoukas, M.; Bedworth, P. V.; Blanchard-Desce, M.; Fort, A.; Hu, Z.-Y.; Marder, S. R.; Perry, J. W.; Runser, C.; Staehelin, M.; Zyss, B. *Science* **1996**, *271*, 335.
- (10) Chen, T.-A.; Jen, A. K.-Y.; Cai, Y. *J. Am. Chem. Soc.* **1995**, *117*, 7295.
- (11) Robello, D. R.; Dao, P. T.; Schildkraut, J. S.; Scozzafava, M.; Urankar, E. J.; Willand, C. S. *Chem. Mater.* **1995**, *7*, 284.
- (12) Verbiest, T.; Burland, D. M.; Jurich, M. C.; Lee, V. Y.; Miller, R. D.; Volksen, W. *Science* **1995**, *268*, 1604.
- (13) Sekkat, Z.; Kang, C.-S.; Aust, E. F.; Wegner, G.; Knoll, W. *Chem. Mater.* **1995**, *7*, 142.
- (14) Singer, K. D.; Kuzyk, M. G.; Sohn, J. E. *J. Opt. Soc. Am. B* **1987**, *4*, 968.
- (15) Li, D.; Ratner, M. A.; Marks, T. J.; Zhang, C.; Yang, J.; Wong, G. K. *J. Am. Chem. Soc.* **1990**, *112*, 7389.
- (16) Yitzchaik, S.; Roscoe, S. B.; Kakkar, A. K.; Allan, D. S.; Marks, T. J.; Xu, Z.; Zhang, T.; Lin, W.; Wong, G. K. *J. Phys. Chem.* **1993**, *97*, 6958.
- (17) Kakkar, A. K.; Yitzchaik, S.; Roscoe, S. B.; Kubota, F.; Allan, D. S.; Marks, T. J.; Lin, W.; Wong, G. K. *Langmuir* **1993**, *9*, 388.
- (18) Lee, H.; Hong, H. G.; Mallouk, T. E.; Kepley, L. J. *J. Am. Chem. Soc.* **1988**, *110*, 618.
- (19) Lee, H.; Mallouk, T. E.; Kepley, L. J.; Hong, H. G.; Akhter, S. *J. Phys. Chem.* **1988**, *92*, 2597.
- (20) Hong, H. G.; Sackett, D. D.; Mallouk, T. E. *Chem. Mater.* **1991**, *3*, 521.
- (21) Putvinski, T. M.; Schilling, M. L.; Katz, H. E.; Chidsey, C. E. D.; Muijsce, A. M.; Emerson, A. B. *Langmuir* **1990**, *6*, 1567.
- (22) Katz, H. E.; Scheller, G.; Putvinski, T. M.; Schilling, M. L.; Wilson, W. L.; Chidsey, C. E. D. *Science* **1991**, *254*, 1485.

- (1) Prasad, P.; Williams, D. J. *Introduction to Nonlinear Optical Effects in Molecules and Polymers*; Wiley: New York, 1991.
- (2) Marder, S. R.; Stucky, G. D.; Sohn, J. E., Eds. *Materials for Nonlinear Optics: Chemical Perspectives*; ACS Symposium Series 455; American Chemical Society: Washington, DC, 1991.
- (3) Kanis, D. R.; Ratner, M. A.; Marks, T. J. *Chem. Rev.* **1994**, *94*, 195.
- (4) Zyss, J. *Molecular Nonlinear Optics*; Academic Press: San Diego, CA, 1994.
- (5) Burland, D. M.; Miller, R. D.; Walsh, C. A. *Chem. Rev.* **1994**, *94*, 31.
- (6) Dalton, L. R.; Harper, A. W.; Ghosn, R.; Steier, W. H.; Ziari, M.; Fetterman, H.; Shi, Y.; Mustachic, R. V.; Jen, A. K.-Y.; Shea, K. J. *Chem. Mater.* **1995**, *7*, 1060.

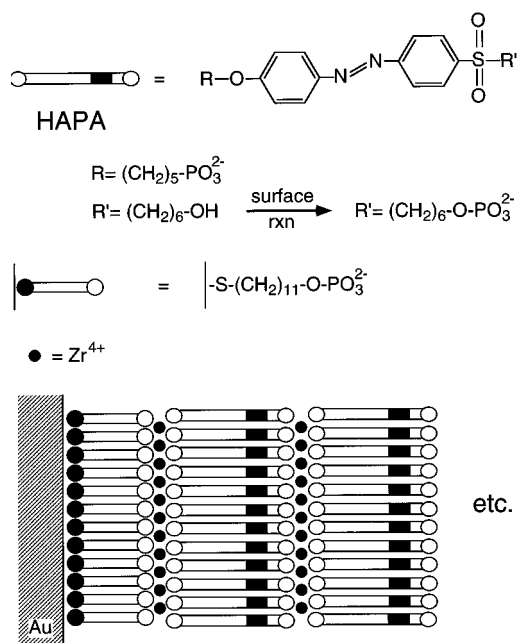


Figure 1. Schematic diagram for the construction of noncentrosymmetric ZP multilayer films. The ZP films are created on vapor-deposited gold substrates that have been first primed with a self-assembled monolayer of phosphorylated MUD. Exposure of the zirconated surface to a solution of the nonlinear optical compound HAPA following the procedure of Katz and co-workers led to noncentrosymmetric multilayer films that exhibited large nonlinear optical responses.

Microscopic measurements have shown that the ZP films are not as highly ordered and oriented as other self-assembled systems such as alkanethiol monolayers.²⁵ We have recently reported the incorporation of azobenzene chromophores into ZP multilayers for the creation of ultrathin films of variable index of refraction.²⁶

In this paper, we describe the synthesis, structural characterization, and nonlinear optical response of noncentrosymmetric ZP azobenzene multilayer films that incorporate the asymmetric nonlinear optical chromophore [5-[4-[[4-[(6-hydroxyhexyl)sulfonyl]phenyl]azo]phenyl]pentoxy]phosphonic acid (HAPA) (Figure 1). The structural characterization of these ultrathin films is accomplished using a combination of optical techniques: polarization/modulation Fourier transform infrared reflection absorption spectroscopy (PM-FTIRRAS), surface plasmon resonance (SPR) measurements of film thickness, and optical second harmonic generation (SHG). An electro-optic coefficient for the ultrathin films is measured with a series of modulated SPR experiments from ZP monolayers that have been incorporated into air-gap capacitors.

A second application area for NLO-active organic molecules has been in the creation of optical probes for the study of interfacial processes. SHG measurements of NLO-active organic compounds that have been incorporated into solid/liquid, liquid/liquid, and liquid/air interfaces have yielded valuable information on adsorption, diffusion, aggregation, and reaction at these interfaces.^{7,27} In an electrochemical environment, the use of nonlinear optical methods can also provide information about the

interfacial electrostatic fields.²⁷ The electric field strength and field profile within ultrathin organic films at charged interfaces is currently not well-characterized, even though the variation of the potential through the ultrathin dielectric layer controls the electrochemical behavior of species incorporated into the interface.^{28–30} One NLO method that has been employed is the characterization of charged interfaces with electric field-induced second harmonic generation (EFISH).^{27,31–33} In principle, the interfacial electric fields can also be monitored via the molecular linear electro-optical response. To date, only a few attempts to measure the electric field strength within adsorbed monolayers at charged electrode surfaces based on electrochromic shift effects have been reported.^{34–37} In this paper we report the first application of the linear electro-optical effect to study in situ the electrostatic fields within ultrathin organic monolayers at electrochemical interfaces. The electro-optical responses of the noncentrosymmetric ZP azobenzene monolayers incorporated into air-gap capacitors and electrochemical interfaces are compared in order to determine the electric field strength within the ZP films at the electrode surface.

EXPERIMENTAL CONSIDERATIONS

Materials. 2,4,6-Collidine (99%), phosphorus oxychloride (99%), zirconyl chloride octahydrate (98%), anhydrous octane (99+%), anhydrous tetrahydrofuran (THF) (99.9%), dihexadecyl phosphate (DHP) (99%), sodium sulfate, potassium carbonate, and lithium aluminum hydride (1 M in THF) were obtained from the Aldrich Chemical Co. Other reactants and solvents included (10-carbomethoxydecyl)dimethylchlorosilane (United Chemical Technologies), tetrabutylammonium bromide (99+%) (Fluka), methylene chloride, UV grade acetonitrile (Burdick and Jackson), ethyl acetate (Fisher), and absolute ethanol (Pharmco). All chemicals were used as received. Mercaptoundecanol (MUD) and 1,10-decanediylbis(phosphonate) (DBP) were synthesized as described previously.³⁸ All aqueous solutions were prepared from 18 MΩ Millipore-filtered water.

HAPA Synthesis. The synthesis of HAPA pictured in Figure 2 is described in detail.

(1) 4-[(6-Hydroxyhexyl)thio]nitrobenzene. In a 250 mL round-bottom flask containing 150 mL of absolute ethanol was placed 2.17 g (14 mmol) of 4-nitrothiophenol (Fluka). The mixture was heated with stirring to dissolve all of the solid. To this solution was slowly added 5.2 mL (14 mmol) of 21 wt % sodium ethoxide in ethanol (Aldrich). The resulting deep red solution was stirred in a nitrogen atmosphere for 10 min. Next, 1.70 mL (13 mmol) of 6-bromo-1-hexanol (Aldrich) was added to the solution. The mixture was refluxed for 12 h until the reaction was complete as determined by TLC in ethyl acetate. The solution was concentrated to half the volume by rotary evaporation and

(23) Katz, H. E.; Wilson, W. L.; Scheller, G. *J. Am. Chem. Soc.* **1994**, *116*, 6636.

(24) Katz, H. E. *Chem. Mater.* **1994**, *6*, 2227.

(25) Ulman, A. *An Introduction to Ultrathin Organic Films*; Academic: New York, 1991.

(26) Hanken, D. G.; Corn, R. M. *Anal. Chem.* **1995**, *67*, 3767.

(27) Corn, R. M.; Higgins, D. A. *Chem. Rev.* **1994**, *94*, 107.

(28) Smith, C. P.; White, H. S. *Anal. Chem.* **1992**, *64*, 2398.

(29) Gao, X.; White, H. S. *J. Electroanal. Chem.* **1995**, *389*, 13.

(30) Basame, S. B.; White, H. S. *J. Phys. Chem.* **1995**, *99*, 16430.

(31) Lantz, J. M.; Baba, R.; Corn, R. M. *J. Phys. Chem.* **1993**, *97*, 7392.

(32) Lantz, J. M.; Corn, R. M. *J. Phys. Chem.* **1994**, *98*, 9387.

(33) Lantz, J. M.; Corn, R. M. *J. Phys. Chem.* **1994**, *98*, 4899.

(34) Schmidt, P. H.; Plieth, W. J. *J. Electroanal. Chem.* **1986**, *201*, 163.

(35) Pope, J. M.; Tan, Z.; Kimbrell, S.; Buttry, D. A. *J. Am. Chem. Soc.* **1992**, *114*, 10085.

(36) Franzen, S.; Goldstein, R. F.; Boxer, S. G. *J. Phys. Chem.* **1990**, *94*, 5135.

(37) Lockhart, D. J.; Hammes, S. L.; Franzen, S.; Boxer, S. G. *J. Phys. Chem.* **1991**, *95*, 2217.

(38) Frey, B. L.; Hanken, D. G.; Corn, R. M. *Langmuir* **1993**, *9*, 1815.

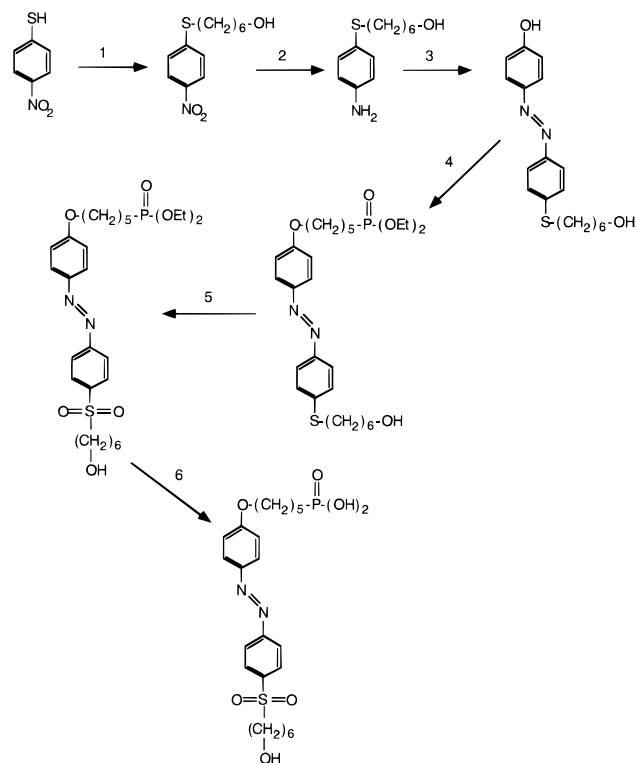


Figure 2. Reaction scheme for the synthesis of the nonlinear optical compound [5-[4-[[4-[(6-hydroxyhexyl)sulfonyl]phenyl]azo]phenyl]pentoxy]phosphonic acid (HAPA). Reaction steps 1–6 are outlined in detail in the text.

added to a separatory funnel containing 10% aqueous K_2CO_3 and ethyl acetate. The organic layer was washed with 5×50 mL portions of 10% aqueous K_2CO_3 and with 2×50 mL portions of saturated aqueous NaCl. The ethyl acetate was subsequently dried with Na_2SO_4 , and the solvent was removed by rotary evaporation to yield 3.02 g (91%) of light yellow solid: 1H NMR (acetone- d_6), δ 1.2–1.8 (m, 8 H), 3.1 (t, 2 H), 3.5 (t, 2 H), 7.2 (d, 2 H), 8.0 (d, 2 H).

(2) 4-[(6-Hydroxyhexyl)thio]aniline. In a 100 mL round-bottom flask containing 30 mL of absolute ethanol was placed 1.5 g (6 mmol) of 4-[(6-hydroxyhexyl)thio]nitrobenzene. To the solution was added 6.6 g (30 mmol) of $SnCl_2 \cdot 2H_2O$ (Mallinckrodt).³⁹ The mixture was refluxed for 12 h until the reaction was complete as determined by TLC in ethyl acetate. The ethanol was removed by rotary evaporation. The resulting yellowish oil was added to a separatory funnel containing 10% aqueous K_2CO_3 and ethyl acetate. The aqueous layer was maintained above pH 8 and extracted with 5×50 mL portions of ethyl acetate. The ethyl acetate was dried with Na_2SO_4 , and the solvent was removed by rotary evaporation to yield 1.14 g (86%) of white solid: 1H NMR ($CDCl_3$), δ 1.2–1.8 (m, 8 H), 3.1 (t, 2 H), 3.4 (t, 2 H), δ 4.2 (s, 2 H), 6.7 (d, 2 H), 7.4 (d, 2 H).

(3) 4-[[4-[(6-Hydroxyhexyl)thio]phenyl]azo]phenol. In a 25 mL flask, 0.56 g (2.5 mmol) of 4-[(6-hydroxyhexyl)thio]aniline was dissolved in 11 mL of hot 10% aqueous HCl with stirring. The solution was rapidly cooled to 0 °C in an ice/salt bath which then became a fine milky suspension. To this mixture, 0.17 g (2.5 mmol) of sodium nitrite (Fisher), dissolved in 2 mL of water, was slowly added in order to keep the solution temperature below 10 °C. Upon addition of the sodium nitrite, the solution turned light

green, and all solid material dissolved. This mixture was stirred at 0 °C for an additional 10 min. In a second 25 mL flask, 0.24 g (2.5 mmol) of phenol (Mallinckrodt) was dissolved in 10 mL of 1% aqueous NaOH and cooled to 0 °C in an ice bath. The diazonium solution was slowly added to the phenolate solution, resulting in a bright red solution. The solution was stirred at 0 °C for 1 h, during which a brown precipitate formed, and then was stirred for 12 h at room temperature. The mixture was added to a separatory funnel containing 10% aqueous HCl and ethyl acetate. The organic layer was washed with 3×50 mL portions of 10% aqueous HCl and with 2×50 mL portions of saturated aqueous NaCl. The ethyl acetate was dried with Na_2SO_4 , and the solvent was removed by rotary evaporation to yield 0.76 g (91%) of an orange-brown solid: 1H NMR (acetone- d_6), δ 1.2–1.8 (m, 8 H), 3.1 (t, 2 H), 3.5 (t, 2 H), 7.0 (d, 2 H), 7.6 (dd, 4 H), 8.1 (d, 2 H).

(4) Diethyl [5-[4-[[4-[(6-Hydroxyhexyl)thio]phenyl]azo]phenyl]pentoxy]phosphonate. In a 100 mL round-bottom flask containing 70 mL of absolute ethanol was placed 0.39 g (1.2 mmol) of 4-[[4-[(6-hydroxyhexyl)thio]phenyl]azo]phenol. The mixture was heated with stirring to dissolve all of the solid. To this solution was slowly added 0.43 mL (1.2 mmol) of 21 wt % sodium ethoxide in ethanol. The deep red solution was stirred in a nitrogen atmosphere for 10 min. Next, 0.32 g (1.1 mmol) of diethyl (5-bromopentyl)phosphonate (Sigma) was added to the solution. The mixture was refluxed for 48 h until the reaction was complete as determined by TLC in ethyl acetate. The solution was concentrated to half the volume by rotary evaporation and added to a separatory funnel containing 10% aqueous K_2CO_3 and ethyl acetate. The organic layer was washed with 7×50 mL portions of 10% aqueous K_2CO_3 and with 2×50 mL portions of saturated aqueous NaCl. The ethyl acetate was dried with Na_2SO_4 , and the solvent was removed by rotary evaporation to yield 0.56 g (87%) of a red paste.

(5) Diethyl [5-[4-[[4-[(6-Hydroxyhexyl)sulfonyl]phenyl]azo]phenyl]pentoxy]phosphonate. In a 100 mL round-bottom flask containing 40 mL of methanol was placed 0.56 g (1.1 mmol) of diethyl [5-[4-[[4-[(6-hydroxyhexyl)thio]phenyl]azo]phenyl]pentoxy]phosphonate. The solution was cooled to 0 °C in an ice bath, and 2 g (3.3 mmol) of oxone (potassium peroxydisulfate) (Aldrich) dissolved in 40 mL of water was slowly added.⁴⁰ The slurry was stirred at 0 °C for 10 min and then was stirred at room temperature. The reaction was complete in 3 h as determined by TLC (1:1 ethyl acetate/acetone). The mixture was then added to a separatory funnel containing 10% aqueous HCl and ethyl acetate. The organic layer was washed with 3×50 mL portions of water and with 2×50 mL portions of saturated aqueous NaCl. The ethyl acetate was dried with Na_2SO_4 , and the solvent was removed by rotary evaporation to yield 0.57 g (96%) of a red paste.

(6) [5-[4-[[4-[(6-Hydroxyhexyl)sulfonyl]phenyl]azo]phenyl]pentoxy]phosphonic Acid. In a 100 mL round-bottom flask containing 30 mL of dry methylene chloride was placed 0.57 g (1.0 mmol) of diethyl [5-[4-[[4-[(6-hydroxyhexyl)sulfonyl]phenyl]azo]phenyl]pentoxy]phosphonate. To this stirred solution was added 0.86 mL (6.5 mmol) of bromotrimethylsilane (Aldrich).⁴¹ The solution was stirred at room temperature under a nitrogen atmosphere for 24 h and was then refluxed for 2 h. The solvent

(40) Trost, B. M.; Curran, D. P. *Tetrahedron Lett.* **1981**, *22*, 1287.

(41) McKenna, C. E.; Higa, M. T.; Cheung, N. H.; McKenna, M.-C. *Tetrahedron Lett.* **1977**, *18*, 155.

(39) Bellamy, F. D.; Ou, K. *Tetrahedron Lett.* **1984**, *25*, 839.

was removed by rotary evaporation, and the excess bromotrimethylsilane was removed under vacuum. Cold 1% aqueous HCl was added to the red paste, and a fine brown precipitate formed. The solid was collected with a glass filter frit and was washed thoroughly with water and ethyl ether. The product was dried under vacuum to yield 0.41 g (80%) of a brown-orange solid: ^1H NMR ($\text{DMSO}-d_6$), δ 1.2–1.75 (m, 14 H), 1.87 (m, 2 H), 3.45 (pt, 4 H), 4.2 (t, 2 H), 7.25 (d, 2 H), 8.0 (d, 2 H), 8.17 (dd, 4 H); IR (KBr) 1602, 1583, 1253, 1137, 1003 cm^{-1} ; UV/visible max (EtOH) 362 nm.

Polarization/Modulation Fourier Transform Infrared Reflection Absorption Spectroscopy (PM-FTIRRAS) Measurements on Gold Substrates. All PM-FTIRRAS spectra were obtained on a Mattson RS-1 spectrometer without a background or reference spectrum by utilizing real-time interferogram sampling electronics that have been described previously.^{42,43} The differential reflectance (% $\Delta R/R$) spectra were converted to absorbance units for comparison with other spectra. Sample spectra in the CH stretching region (3100–2700 cm^{-1}) were obtained with an InSb detector, and spectra in the mid-infrared region (1800–850 cm^{-1}) were obtained with a narrow-band HgCdTe detector. All infrared spectra were acquired at 2 cm^{-1} resolution from 1024 interferometer scans.

SPR and Electro-Optical Measurements on Gold Substrates. The experimental apparatus for conventional scanning surface plasmon resonance measurements was described in detail in a previous paper.⁴⁴ This apparatus measures the reflectivity of p-polarized light from a HeNe laser (632.8 nm, 1 mW, Newport Corp.) from the BK7/Au/ZP film sample as a function of the incident angle, θ . For air-gap electro-optical SPR measurements, the sample setup is pictured in the inset of Figure 7. The ZP-coated thin gold samples (470 Å) were placed in optical contact with a BK7 right-angle prism (Melles Griot) using an index-matching fluid (Type NVH, Cargille Labs). This gold sample was spaced from a second gold electrode (1200 Å of gold deposited on a fused-silica window) by a thin sheet of Mylar dielectric film (DuPont, 14C gauge). A small square was cut out of the Mylar to produce a thin air gap. The air gap was aligned with the incident HeNe laser beam to allow the surface plasmon wave to be evanescent in air upon excitation. The thickness of this gap, assuming the sample to be a parallel-plate capacitor, was estimated from a measurement of the capacitance (BK Precision 820 capacitance meter, Dynascan Corp.). The value for the air gap was calculated to be $\sim 15 \mu\text{m}$ for the sample in Figure 7. An ac electric field with a peak-to-peak amplitude of 10–50 V at a frequency of 1–10 kHz (Model 501 ac power source, Elgar Corp.) was applied to the sample cell to produce an oscillating electric field on the order of 10^4 V/cm . This modulation produced a corresponding modulation in the reflectivity due to the Pockel's effect which was detected by use of a photodiode (Hamamatsu) and a lock-in amplifier (SR510, Stanford Research Systems).

For in situ electro-optical measurements, the sample setup is pictured in the inset of Figure 8. The ZP-coated thin gold samples (470 Å) formed on SF10 glass slides (Schott) were placed in optical contact with an SF10 equilateral prism (Ealing Electro-Optics, Inc.) using an index-matching fluid (1-iodonaphthalene,

Aldrich). The sample cell consisted of a Teflon electrochemical cell that was pressed against the ZP-coated thin gold sample by use of a viton o-ring for a water-tight seal. The electrochemical cell was made to incorporate two electrodes and a nitrogen line for solution purging. A three-electrode assembly was formed with the ZP-coated gold sample as the working electrode, a saturated calomel reference electrode, and a platinum counter electrode. The potential was controlled by a potentiostat (EG&G Model 173 potentiostat/galvanostat) and a voltage controller (EG&G Model 175 Universal Programmer). All in situ electrochemical experiments were carried out using 0.2 M tetrabutylammonium bromide as the electrolyte. Cyclic voltammograms were recorded in the potential region -0.4 to 0.7 V vs SCE. In this region, no faradaic processes occurred for the ZP samples. The potential was fixed to 0.0 V vs SCE, and a small sinusoidal modulation ($\pm 25 \text{ mV}$, 1 kHz, Model 5100B function generator, Krohn & Hite) was applied to the electrochemical cell. This modulation produced a corresponding modulation in the reflectivity due to the Pockel's effect which was detected by use of a photodiode and a lock-in amplifier.

Theoretical Fresnel fits to the electro-optical data were calculated by subtracting two surface plasmon theory curves which differed only by small changes in the real component of the dielectric constant of the ZP film. Air-gap experiments were fit using a five-phase model (BK7, Au, phosphorylated MUD, HAPA, air).^{26,44,45} In the in situ case, a background signal due to the electro-optical modulation of the surface gold layer (0.5 Å) was compensated for in the theory calculations by using a seven-phase model [SF10, Au, Au (0.5 Å), phosphorylated MUD, HAPA, DHP, water]. This background signal was not observed within the signal-to-noise ratio in the air-gap electro-optical experiments.

UV/Visible Absorption and Ellipsometry Measurements on Fused-Silica Substrates. UV/visible absorption spectra were obtained on a Hewlett-Packard Model 8452A diode array spectrophotometer. Micromolar solutions of HAPA in ethanol exhibited an absorption maximum at 362 nm. The absorption is associated with the main charge transfer transition for this molecule. On fused-silica substrates, the position of this transition red-shifted slightly to 365 nm upon incorporation into the ZP multilayer films, indicating that the HAPA chromophores do not significantly interact within the films. The amount of absorbance at 365 nm increased in a linear fashion with the number of HAPA layers for all ZP multilayer samples. Ellipsometry measurements for the HAPA films on fused-silica substrates were obtained with a Rudolph Research Model AutoEL II ellipsometer employing 633 nm light. Theoretical Fresnel fits to the data were calculated as described previously.²⁶

Second Harmonic Generation Measurements on Fused-Silica Substrates. Second harmonic generation measurements for ZP films deposited onto a primer layer on fused-silica substrates were made by employing a Nd:YAG pumped dye laser (10 ns pulse width, 10 Hz repetition rate) and an experimental configuration described previously.⁴⁶ The fundamental input wavelength of 730 nm was focused onto the silica surface at an incident angle of 60° , and the second harmonic light at 365 nm was measured in reflection from the top silica surface. Filters and a 0.175 M monochromator were used to remove any reflected fundamental light. The SHG signal was detected with a photo-

(42) Green, M. J.; Barner, B. J.; Corn, R. M. *Rev. Sci. Instrum.* **1991**, *62*, 1426.

(43) Barner, B. J.; Green, M. J.; Saez, E. I.; Corn, R. M. *Anal. Chem.* **1991**, *63*, 55.

(44) Jordan, C. E.; Frey, B. L.; Kornguth, S.; Corn, R. M. *Langmuir* **1994**, *10*, 3642.

(45) Hansen, W. N. *J. Opt. Soc. Am.* **1968**, *58*, 380.

(46) Higgins, D. A.; Byerly, S. K.; Abrams, M. B.; Corn, R. M. *J. Phys. Chem.* **1991**, *95*, 6984.

multiplier tube, and the output was averaged with a boxcar averager. Orientation measurements for the HAPA films, which were determined from polarization dependence experiments, are obtained by measuring the intensity of the s-polarized and p-polarized SHG signals as a function of the polarization of the incident fundamental light.^{47–49}

RESULTS AND DISCUSSION

A. Noncentrosymmetric HAPA Multilayer Films at Gold Surfaces. Ultrathin (<50 nm) noncentrosymmetric organic films were formed on gold substrates by the sequential deposition of self-assembled ZP monolayers of the molecule HAPA (see Figure 1). The HAPA molecule contains an azobenzene NLO chromophore with sulfonyl electron-accepting and phenyl ether electron-donating groups (with an absorption maximum at 365 nm) and is terminated with a phosphonic acid on one end and an alcohol functional group on the other. This organic chromophore was specifically chosen over others that contain amine electron-donating substituents because its absorption maximum is blue-shifted considerably from the visible region. This reduced the possibility of resonant contributions to the electro-optical measurements. A noncentrosymmetric HAPA multilayer is formed by the method outlined by Katz et al.,^{21–24} in which HAPA adsorbs as a self-assembled monolayer on a Zr^{4+} ion-coated substrate via the phosphonic acid group, and then the terminal alcohol groups on the other end of the molecule are converted to phosphates which can bind a new monolayer of Zr^{4+} ions for the adsorption of a subsequent HAPA monolayer. Films of up to 10 HAPA monolayers were created by this sequential self-assembly process. These ultrathin noncentrosymmetric HAPA films are used in section C for the study of electric fields within organic films at electrode surfaces via the electro-optical effect.

Multilayer films of HAPA were formed on vapor-deposited gold substrates using a primer monolayer and deposition conditions that were optimized previously.^{26,38} The primer layer for the gold substrates consisted of a self-assembled monolayer of MUD, in which the terminal hydroxy group is converted to a phosphate species via a surface reaction.³⁸ This primer layer is then exposed to an aqueous solution of Zr^{4+} ions. As reported previously, PM-FTIRRAS measurements show that this primer monolayer has a well-organized zirconium phosphate structure that can serve as the basis for the creation of ZP multilayer films.³⁸ A HAPA monolayer is self-assembled onto this primer layer by exposure to a 0.5 mM ethanolic HAPA solution over a period of 16 h. This monolayer adsorption is followed by phosphorylation of the terminal alcohol groups with phosphorus oxychloride and then subsequent exposure to an aqueous Zr^{4+} solution to form a Zr^{4+} -terminated monolayer. Repetition of these steps leads to the formation of multilayer HAPA films. For the electro-optical studies at electrochemical surfaces, a terminal monolayer of DHP was self-assembled onto the ZP monolayer in order to produce a very hydrophobic surface that would reduce the penetration of electrolyte into the film. Each of the deposition steps in the multilayer film formation process was verified with a combination of PM-FTIRRAS and SPR measurements.

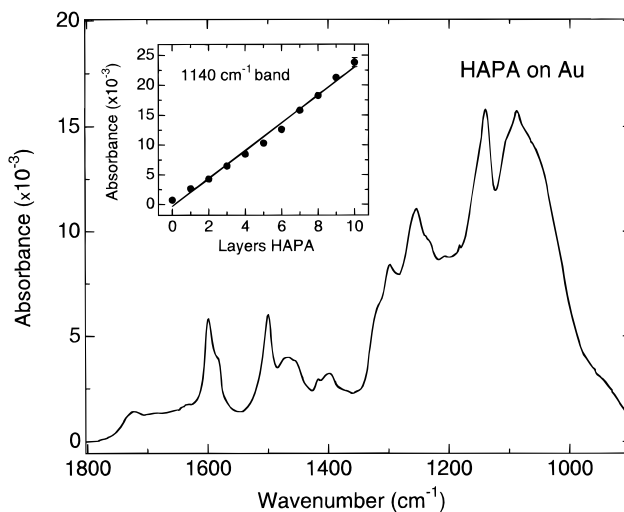


Figure 3. Mid-infrared region of the PM-FTIRRAS spectrum of a seven-layer ZP/HAPA film on a vapor-deposited thin gold film. The gold surface was primed with a self-assembled monolayer of phosphorylated MUD before the formation of the ZP films. The frequencies and band assignments for the spectrum are listed in Table 1. The inset graph plots the intensity of the 1140 cm^{-1} symmetric sulfonyl stretching band as a function of the number of HAPA monolayers during the formation of a 10-layer ZP film. The straight line is a linear fit to the data. This linear dependence is observed for all of the bands listed in Table 1.

Table 1. Vibrational Band Frequencies and Assignments for the HAPA Multilayers^{65–68}

frequency (cm^{-1})	band	assignment
HAPA Film		
2930 ± 1	$\nu_a(CH_2)$	methylene stretch
2855	$\nu_s(CH_2)$	methylene stretch
1599	$\nu_{8a}(CC)^a$	ring stretch
1585	$\nu_{8b}(CC)^a$	ring stretch
1500	$\nu_{19a}(CC)^a$	ring stretch
1469	$\delta(CH_2), \nu_{19b}(CC)^a$	CH_2 scissoring deformation ring stretch
1400	$\delta(\alpha-CH_2)$	$\alpha-CH_2$ scissoring deformation
1298	$\nu_a(SO_2)$	sulfonyl stretch
1254	$\nu_a(COC)$	phenyl ether stretch
1140	$\nu_s(SO_2)$	sulfonyl stretch
1088	$\nu_a(PO_3^{3-}), \nu_a(PO_4^{2-})$	phosphonate/phosphate stretch

^a Frequency modes and assignments follow the numbering convention of Wilson for p-substituted benzenes and azobenzenes.^{50,69,70}

The PM-FTIRRAS spectra of the ultrathin films yield information about the molecular structure and orientation within the self-assembled multilayer. In previous papers, we have demonstrated that PM-FTIRRAS is particularly well-suited to studying the formation of ZP multilayer films on gold surfaces.^{26,38} The mid-infrared region of the PM-FTIRRAS spectrum for a seven-layer HAPA film self-assembled onto a primer layer on a gold surface is shown in Figure 3. The frequencies and assignments of the various infrared bands are listed in Table 1. Absorption bands at 1599, 1585, and 1500 cm^{-1} are assigned to the azobenzene functionality by comparison with bulk infrared spectra.⁵⁰ The absorption band at 1088 cm^{-1} has been observed previously in other ZP multilayer films and is attributed to the phosphate and phosphonate groups in the HAPA multilayer.^{26,38} Two additional

(47) Mizrahi, V.; Sipe, J. E. *J. Opt. Soc. Am. B* **1988**, *5*, 660.

(48) Heinz, T. F. In *Nonlinear Surface Electromagnetic Phenomena*; Ponath, H. E., Stegeman, G. I., Eds.; North-Holland: Amsterdam, 1991.

(49) Corn, R. M.; Higgins, D. A. In *Characterization of Organic Thin Films*; Ulman, A., Ed.; Butterworth-Heinemann: Woburn, MA, 1995.

(50) Klima, M. I.; Kotov, A. V.; Gribov, L. A. *J. Struct. Chem.* **1972**, *13*, 987.

prominent bands appear at 1298 and 1140 cm^{-1} and are assigned as the sulfonyl antisymmetric and symmetric stretching modes, respectively. The presence of these two bands in the PM-FTIRRAS spectrum suggests that the NLO chromophores in the HAPA multilayer film are not oriented completely normal to the gold surface. If they were, then these vibrational modes would be parallel to the gold surface and would not be observed due to the surface selection rules at metal surfaces.⁵¹ The appearance of these bands indicates that there is a significant amount of tilting of the azobenzene chromophores in the HAPA multilayer film. This effect has been observed previously in other azobenzene/ZP films²⁶ and has been attributed to the inability of these films to form highly packed ZP multilayers due to the mismatch of the azo dye substituent size and the lattice spacing of the inorganic regions in the ZP film.⁵² The amount of tilt does not change as a function of the number of HAPA monolayers since the relative band intensities in the infrared spectrum of the HAPA film did not change during the multilayer deposition process. In Figure 3, the inset graph plots the intensity of the 1140 cm^{-1} band as a function of the number of HAPA monolayers during the formation of a multilayer film. The linear increase in the intensity of this band indicates that each additional self-assembly step creates an additional HAPA monolayer with an equivalent molecular structure and packing density. This linear increase was observed for all of the bands listed in Table 1.

In conjunction with the PM-FTIRRAS measurements, SPR measurements were used to provide quantitative information on the thickness of the HAPA multilayer films. We have demonstrated previously the utility of the SPR method for assessing film thicknesses of ZP multilayers.²⁶ Following the approach used in our previous paper, the shifts that occurred in the SPR angle ($\Delta\theta$) were measured during the sequential deposition of a HAPA multilayer film on a thin (470 Å) gold substrate. Figure 4 plots the shifts in the SPR angle that were obtained after the addition of each self-assembled HAPA monolayer in a 10-layer HAPA film. Five phase complex Fresnel calculations are used to interpret these shifts in SPR angle;^{26,44,45} these calculations used a value of 1.65 for the index of refraction of the ultrathin HAPA multilayer, which was determined from ellipsometric measurements of HAPA films on fused-silica substrates (see below). This index of refraction is consistent with that observed for similar azobenzene ZP films.²⁶ With these Fresnel calculations, the shifts in the SPR angle can be used to ascertain an average film thickness for the HAPA monolayers; the solid and dashed lines in Figure 4 are theoretical curves generated from the Fresnel calculations for monolayer thicknesses of 26, 27, and 28 Å. The fit to the experimental data indicates that the HAPA monolayers in the ZP multilayer films exhibit a thickness of 27 ± 0.5 Å. A space filling model of the HAPA multilayer ZP film in which the azobenzene functionality is oriented perpendicular to the surface and the two methylene chains are in all-trans configurations predicts a Zr^{4+} /HAPA monolayer thickness of approximately 31–32 Å.^{53,54} The experimentally determined value of 27 Å is in agreement with the chromophore tilting observed in the PM-FTIRRAS spectra of the multilayer films.

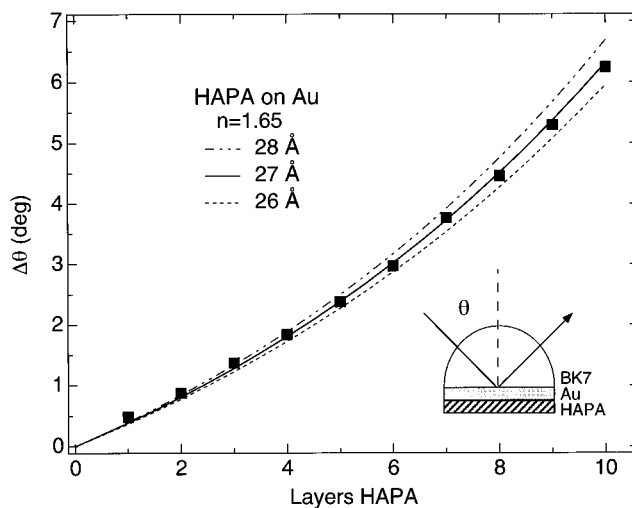


Figure 4. Shifts in the SPR angle ($\Delta\theta$) measured during the formation of a 10-monolayer ZP/HAPA film onto a primer layer on a thin (470 Å) gold film that is in optical contact with a BK7 prism. The reflectivity of p-polarized light at 632.8 nm from the BK7/Au/HAPA sample is monitored as a function of incident angle, θ (see inset). The shifts $\Delta\theta$ were determined from SPR reflectivity curves with the SPR angle of the primer layer, denoted as the "0 layer" surface and defined as $\Delta\theta = 0$. The three lines in the figure are the results of complex Fresnel calculations using an index of refraction of 1.65 (as determined from ellipsometric experiments) for the ZP multilayer and a HAPA monolayer thickness of 26, 27, or 28 Å. From the experimental data, a HAPA monolayer thickness of 27 ± 0.5 Å is determined.

B. Noncentrosymmetric HAPA Multilayer Films at Silica Surfaces. In conjunction with the HAPA multilayers formed on gold substrates, noncentrosymmetric HAPA multilayers were formed on fused-silica substrates in order to characterize the linear and nonlinear optical properties of the thin films. The primer layer on the transparent substrates consisted of a self-assembled monolayer of (10-carbomethoxydecyl)dimethylchlorosilane that was chemically converted to a phosphate species on the surface as detailed previously.²⁶ This phosphate-terminated surface was then exposed to an aqueous solution of Zr^{4+} . Once the initial Zr^{4+} -coated surface was created, the adsorption of the HAPA monolayers was performed in a fashion identical to those on the gold substrates. The characterization of the ZP multilayer films on the silica substrates employed a combination of UV/visible absorption, ellipsometry, and SHG measurements.

The UV/visible absorption spectrum for a four-layer HAPA film is plotted in Figure 5. A large charge transfer absorption band is observed at 365 nm; this absorption maximum is red-shifted by only 3 nm from its value in dilute ethanolic solutions. The small shift indicates that there is very little interaction between the NLO chromophores in the ZP multilayer films. As detailed in previous papers, the sensitivity of the surface plasmon resonance technique depends on both the thickness and index of refraction of the absorbed film.^{26,44} Therefore, different combinations of thickness and index of refraction can be used to fit measured shifts in the SPR angle. To assist with the interpretation of the SPR measurements at gold surfaces, ellipsometric measurements at 633 nm were performed on 5, 8, and 10-multilayer HAPA films on silica substrates in order to determine a film index of refraction of 1.65 ± 0.04 . A thickness per HAPA monolayer of 27 ± 6 Å was also determined from the ellipsometric data. The variability of these thickness values on silica substrates was significantly greater than

(51) Pearce, H. A.; Sheppard, N. *Surf. Sci.* **1976**, *59*, 205.

(52) Alberti, G.; Costantino, U.; Marmottini, F.; Vivani, R.; Zappelli, P. *Angew. Chem., Int. Ed. Engl.* **1993**, *32*, 1357.

(53) Dines, M. B.; DiGiacomo, P. M. *Inorg. Chem.* **1981**, *20*, 92.

(54) Zeppenfeld, A. C.; Fiddler, S. L.; Ham, W. K.; Klopfenstein, B. J.; Page, C. *J. Am. Chem. Soc.* **1994**, *116*, 9158.

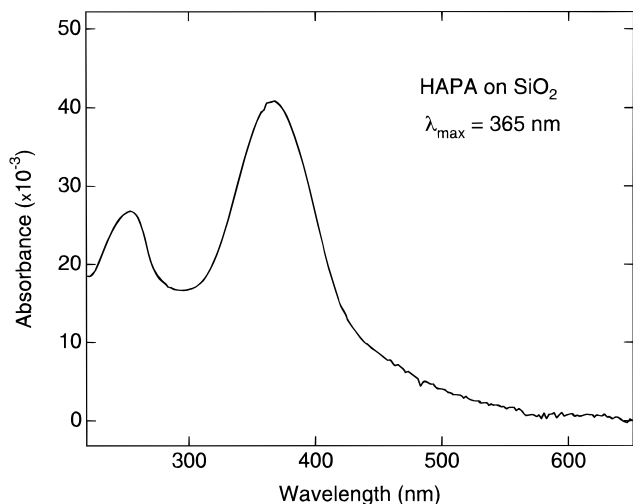


Figure 5. Surface UV/visible absorption spectrum for a four-layer ZP/HAPA film formed onto a primer layer on a fused-silica surface. The absorption maximum at 365 nm is associated with the charge transfer transition for this molecule. The absorption maximum is slightly shifted from the solution spectrum, indicating only a small amount of interaction between HAPA chromophores takes place in the ZP film.

that observed for the ZP multilayer films created on gold surfaces.²⁶ This difference reflects the variability in the primer layer formation on the fused-silica substrates.

The noncentrosymmetric nature of the HAPA multilayer films on silica substrates was assessed with resonant optical SHG measurements. SHG measurements have been made previously on ZP multilayer films.^{22,23} The SHG measurements in this work are performed at a fundamental wavelength of 730 nm. At this wavelength, the measurements are in resonance with the HAPA charge transfer transition at the second harmonic wavelength of 365 nm. We have previously used the resonant-enhanced SHG from similar NLO azobenzene chromophores to study adsorption to liquid/liquid interfaces.^{55,56} Figure 6 plots the measured second harmonic signal as a function of the number of HAPA monolayers in a five-layer ZP film on a fused silica substrate. The solid line in the figure is a quadratic fit to the data that arises from the dependence of the SHG signal on the square of the surface concentration of oriented SHG-active chromophores at the interface. These SHG measurements clearly indicate that the self-assembly of the HAPA multilayers produces a uniformly noncentrosymmetric ultrathin organic film.

In addition to the magnitude of the SHG from the HAPA multilayer films, the polarization dependence of the signal from the multilayers was used to examine the average orientation of the NLO chromophores in the films. This polarization dependence was determined by measuring the intensity of the s-polarized and p-polarized SHG signals as a function of the polarization of the incident fundamental light.^{47–49} An analysis of this polarization dependence (not shown) resulted in the determination of an orientation parameter, $D = \langle \cos^3 \theta \rangle / \langle \cos \theta \rangle$, where θ is the angle between the primary axis of the NLO chromophore (in this case the long axis of the HAPA molecule) and the surface normal.⁵⁷ A value of $D = 0.79 \pm 0.03$ was obtained for the HAPA multilayer films on silica substrates; this value corresponds to an

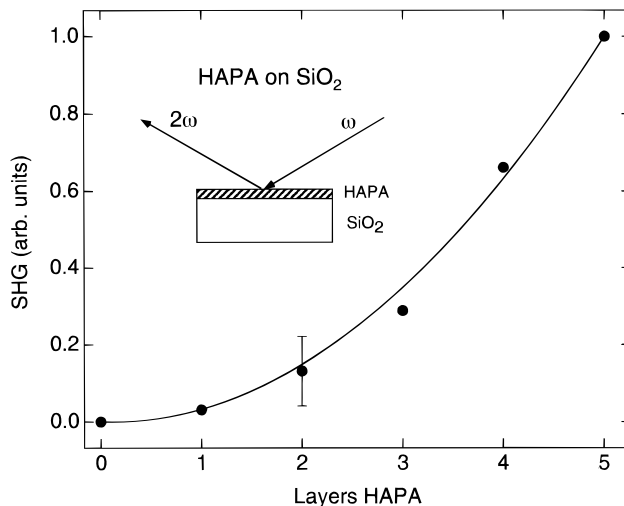


Figure 6. Observed second harmonic generation intensity obtained for a five-layer ZP/HAPA film. The HAPA multilayer for these measurements is self-assembled onto a phosphorylated silane primer layer on a fused-silica substrate. A fundamental input wavelength of 730 nm is employed to be in resonance with the HAPA charge transfer electronic transition at the second harmonic wavelength of 365 nm. The SHG signal at 365 nm is obtained in a reflection geometry from the top surface. (See inset). The solid line is a quadratic fit to the observed data.

angle θ of $27 \pm 2^\circ$ from the surface normal if all of the HAPA molecules in the film have the same tilt angle (i.e., if $\langle \cos^3 \theta \rangle \approx \cos^3 \langle \theta \rangle$ and $\langle \cos \theta \rangle \approx \cos \langle \theta \rangle$). The orientation parameter and tilt angle are consistent with the average thickness as determined from SPR experiments and the observed PM-FTIRAS spectra of HAPA multilayers on gold surfaces.

C. Electro-Optic Coefficient of a HAPA Monolayer. Determination of the linear electro-optical properties of a HAPA monolayer film was accomplished by the use of modulated surface plasmon resonance measurements. This method has been used previously for determination of the electro-optic coefficients of ultrathin Langmuir–Blodgett NLO organic films by Cross and co-workers,^{58,59} and micrometer-thick NLO poled polymer films by Sekkat et al.¹³ In these experiments, the ultrathin NLO organic film is deposited onto a thin (470 Å) gold film that serves as one electrode of an air-gap capacitor (see the inset in Figure 7). An external ac voltage (on the order of 10–50 V with a frequency of 1–10 kHz) is applied to the capacitor in order to create an oscillating electrostatic field on the order of 10^4 V/cm that modulates the index of refraction of the ultrathin NLO organic film via the electro-optical effect. This change in the index of refraction results in a shift of the SPR angle that can be observed by detecting the modulated change in reflectivity as a function of incident angle, θ .

Figure 7 plots the modulated change in reflectivity ($\Delta\%R$) as a function of incident angle near the surface plasmon angle (θ_{sp}) for a single HAPA monolayer film. This signal was obtained from application across the air gap of a ± 15 V sinusoidal voltage at a frequency of 10 kHz. The thickness of the air gap in the capacitor in this experiment was determined from capacitance measure-

(55) Naujok, R. R.; Higgins, D. A.; Hanken, D. G.; Corn, R. M. *J. Chem. Soc., Faraday Trans.* **1995**, *91*, 1411.

(56) Naujok, R. R.; Paul, H. J.; Corn, R. M. *J. Phys. Chem.* **1996**, *100*, 10497.

(57) Heinz, T. F.; Tom, H. W.; Shen, Y. R. *Phys. Rev. A* **1983**, *28*, 1883.

(58) Cross, G. H.; Girling, I. R.; Peterson, I. R.; Cade, N. A.; Earls, J. D. *Electron. Lett.* **1986**, *22*, 1111.

(59) Cross, G. H.; Girling, I. R.; Peterson, I. R.; Cade, N. A.; Earls, J. D. *J. Opt. Soc. Am. B* **1987**, *4*, 962.

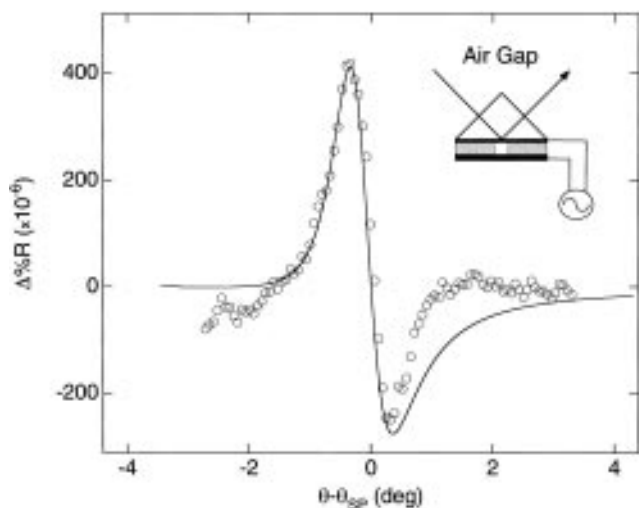


Figure 7. Differential reflectivity ($\Delta\%R$) obtained by modulated surface plasmon resonance measurements in air for a ZP film consisting of a monolayer ZP/HAPA film formed onto a primer layer on a thin gold film. This signal is attributed to a modulation in the dielectric constants of the HAPA monolayer through the nonlinear electro-optical (Pockel's) effect. The sample for this experiment shown in the inset of the figure consists of a thin Mylar dielectric film which is pressed between the ZP-modified gold sample and a second gold electrode. A small square is cut out of the Mylar so the surface plasmon wave is evanescent in air upon excitation. The thickness of the resulting air gap is calculated to be $15\ \mu\text{m}$. Electrical contact is made to the two gold surfaces, and a sinusoidal wave form is applied across the gap ($\pm 15\ \text{V}$, $10\ \text{kHz}$). The differential reflectivity caused by this modulation is recorded as a function of the incident angle θ . The solid line in the figure is a complex Fresnel fit to the data obtained by varying the real component of the dielectric constant of the HAPA layer.

ments to be $15\ \mu\text{m}$. A static or zero frequency dielectric constant of 6 was assumed for the ZP/HAPA monolayer films. This value was chosen to match the experimentally determined dielectric constant for similar NLO azo dye multilayer ZP films reported by Katz et al.^{24,60} The conditions of this experiment correspond to an electric field strength of $3.3 \times 10^3\ \text{V/cm}$ within the ZP/HAPA monolayer film. The change in reflectivity at $10\ \text{kHz}$ was obtained by lock-in amplifier detection of the photodiode current (see the Experimental Section for more details) and has the functional form of the derivative of the standard surface plasmon reflectivity curve. The magnitude of the differential reflectivity ($\Delta\%R$) increased linearly with the applied ac voltage for the HAPA sample as expected and was essentially constant over the frequency range of $1\text{--}10\ \text{kHz}$. In addition, no signal was observed in the absence of the HAPA monolayer. The solid line in Figure 7 is a five-phase Fresnel calculation in which the real part of the index of refraction for the HAPA monolayer is varied by $\Delta n = 8.0 \times 10^{-6}$. A similar change in the SPR reflectivity can be obtained by a change in the thickness of the film with applied voltage (Δd), but we assume that all changes are due to index of refraction effects via the electro-optic coefficient. A change in Δn of 8.0×10^{-6} corresponds to an electro-optic coefficient r_{33} of $11\ \text{pm/V}$ at $632.8\ \text{nm}$.¹³ This value of r_{33} is an off-resonance measurement since no absorption of light in the monolayer film occurs at this wavelength. From the value of r_{33} , the surface nonlinear susceptibility $\chi_{zz}^{(2)}(-\omega; \omega, 0)$ for the ZP film is calculated to be $41\ \text{pm/V}$ ($9.7 \times 10^{-8}\ \text{esu}$).^{13,14} The HAPA molecular hyperpolarizability β_{zz} can then be estimated

from $\chi_{zz}^{(2)}$ and the tilt angle of the chromophore units by assuming a number density for the HAPA film on the Au surface.⁵⁵ The estimated value for β_{zz} of $9.3 \times 10^{-29}\ \text{esu}$ at $632.8\ \text{nm}$, while larger than sum-over-state (SOS) and finite-field (FF) theoretical calculations made at $1907\ \text{nm}$ for similar NLO chromophores, is reasonable given the dispersion relationship of β vs wavelength.^{14,61} The magnitude of the electro-optic coefficient in these ZP films is less than LiNbO_3 but is within the range of the values observed in NLO poled polymer films.^{5,9-14} Moreover, the noncentrosymmetric character of the HAPA monolayer did not decrease with time, as is often the case for the polymer systems.

D. Electric Field Measurements at Electrochemical Surfaces. As an example of the utility of the noncentrosymmetric HAPA multilayer films, a HAPA monolayer was formed at a gold electrode surface in order to measure the electrostatic fields in an electrochemical environment. Electric fields at electrochemical interfaces are thought to vary from 10^3 to $10^8\ \text{V/cm}$, depending on the exact nature of the electrode surface.^{62,63} Previous optical studies have used electroreflectance,³⁴ fluorescence,³⁵⁻³⁷ and SHG measurements^{27,31-33} to examine the electric fields at electrochemical interfaces. When the electrode is coated with an ultrathin organic film, the electric fields are expected to be significantly lower than in the case of a simple metal/electrolyte interface.²⁸⁻³⁰ Nevertheless, these electric field strengths can be monitored via the electro-optical effect for the noncentrosymmetric HAPA multilayers.

A rough schematic diagram of the experiment is pictured in the inset of Figure 8. Instead of an air-gap capacitor, a Teflon cell is pressed against the HAPA-modified gold slide with an o-ring seal. A three-electrode potentiostat with the $470\ \text{\AA}$ thin gold film as the working electrode is used to modulate the potential and interfacial electric fields. Cyclic voltammetry of the HAPA-modified gold slides in $0.2\ \text{M}$ tetrabutylammonium bromide exhibited no faradaic processes in the range from -0.4 to $0.7\ \text{V}$ vs SCE. For the SPR modulation experiments, the electrode potential was fixed to $0.0\ \text{V}$ vs SCE, and a small sinusoidal wave form was applied ($\pm 25\ \text{mV}$ at $1\ \text{kHz}$) to the electrochemical system.

The in situ modulated surface plasmon spectra that are observed from this modulation are plotted in Figure 8. Two modulation experiments are shown in the figure: one for a ZP multilayer that contains HAPA and one that does not. The open circles are the data obtained for a ZP multilayer that does not contain HAPA, but instead consists of a primer monolayer of phosphorylated MUD, followed by two layers of DBP, and one capping layer of DHP. The modulation in the SPR signal in these data results from electro-optical contributions of the gold electrode surface. This effect was not observed in the air-gap experiment to within the signal-to-noise ratio of the experiment, but changes in the optical constants of metal electrode surfaces have been observed previously in electroreflectance measurements.^{62,64} The solid line that fits these data is a seven-phase Fresnel calculation

(61) Ulman, A.; Willand, C. S.; Köhler, W.; Robello, D. R.; Williams, D. J.; Handley, L. *J. Am. Chem. Soc.* **1990**, *112*, 7083.

(62) Kolb, D. M. In *Surface Polaritons*; Agranovich, V. M., Mills, D. L., Eds.; North-Holland: Amsterdam, 1982.

(63) Adamson, A. W. *Physical Chemistry of Surfaces*, 5th ed.; Wiley: New York, 1990.

(64) Kolb, D. M. In *Spectroelectrochemistry: Theory and Practice*; Gale, R. J., Ed.; Plenum Press: New York, 1988.

(65) Bellamy, L. J. *The Infra-red Spectra of Complex Molecules*; Wiley: New York, 1975.

(60) Katz, H. E.; Schilling, M. L. *Chem. Mater.* **1993**, *5*, 1162.

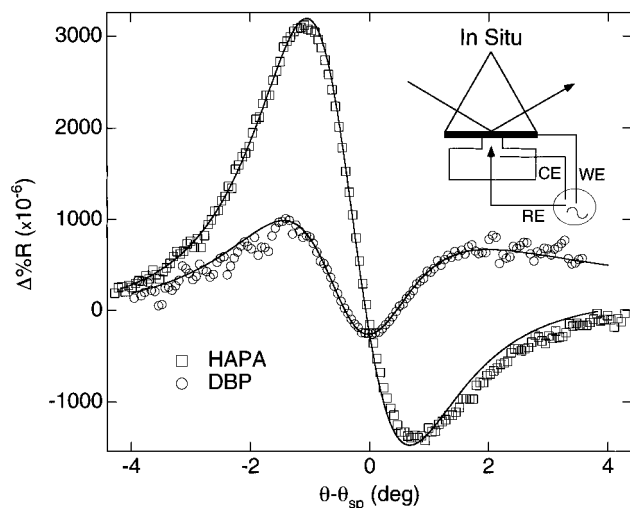


Figure 8. Differential reflectivity ($\Delta\%R$) obtained by modulated surface plasmon resonance measurements made in situ. The sample for this experiment shown in the inset of the figure consists of a Teflon cell which is pressed against the ZP-modified gold sample. A three-electrode assembly is made with the ZP-modified gold sample as the working electrode. A potentiostat controlled the applied potential relative to SCE. The electrolyte consisted of 0.2 M tetrabutylammonium bromide in water. A small sinusoidal wave form (± 25 mV, 1 kHz) was then applied to the cell at a potential where no electrochemistry took place. The open circles are obtained for a ZP film consisting of two monolayers of DBP, and one monolayer of DHP formed onto a primer layer on a thin gold film. This signal results from a modulation in the gold dielectric constants. The open squares are obtained for a ZP film consisting of one monolayer of HAPA and one monolayer of DHP formed onto a primer layer on a thin gold film. The solid lines for both sets of data are complex Fresnel fits obtained by varying the real component of the dielectric constant of the HAPA layer and the gold.

which assumes that the real part of the index of refraction of the first 0.5 \AA of the gold electrode surface changes upon modulation of the electrode potential by an amount $\Delta n = 1.6 \times 10^{-3}$. The thickness of this layer is taken as 0.5 \AA in order to approximate the Thomas–Fermi screening depth of the metal.⁶⁴ Increasing this thickness reduced the size of Δn but had no effect on the shape of the calculated fit. Note that, for these data, the minimum in $\Delta\%R$ occurs at the surface plasmon angle θ_{sp} . This is in contrast to the air-gap capacitor data for the HAPA monolayer (Figure 7).

The second SPR modulation experiment plotted in Figure 8 (the open squares) was obtained for a single-monolayer HAPA film formed on a phosphorylated MUD primer monolayer and capped with a DHP monolayer. The differential reflectivity curve for this sample is significantly different in both shape and magnitude as compared to the curve observed for the DBP sample, with the minimum and maximum in $\Delta\%R$ occurring above and below θ_{sp} as in the case for the air-gap capacitor experiments. The solid line that fits the data is a seven-phase Fresnel fit taking both the modulation of the index of refraction of the HAPA

monolayer and the modulation of the index of refraction of the gold surface into account. This theoretical fit yields a value for the change in index of refraction for the HAPA monolayer of $\Delta n = 3.3 \times 10^{-5}$. This value is a factor of 4 greater than that measured in the air-gap experiment and therefore corresponds to a change in electric field strength during potential modulation of roughly $1 \times 10^4 \text{ V/cm}$ within the ultrathin organic film. This value is close to that expected for a potential modulation of ± 25 mV across an ultrathin organic film with a thickness of 70 \AA (which is the thickness expected for the MUD/HAPA/DHP multilayer). The observation of an electric field strength within the multilayer of $1 \times 10^4 \text{ V/cm}$ indicates that there is only minimal electrolyte penetration into this ZP multilayer in the electrochemical environment. The magnitude of the electric field strength is similar to that determined by Pope et al. for fluorescent hemicyanine chromophores imbedded in self-assembled monolayers on roughened silver electrodes, although their measurements actually probed the diffuse region of the interfacial electric double layer.³⁵

SUMMARY AND CONCLUSIONS

In summary, the experiments described in this paper demonstrate that ultrathin noncentrosymmetric ZP films that incorporate the nonlinear optical chromophore HAPA can be formed on gold and fused silica substrates. A combination of PM-FTIRRAS, SPR, and SHG measurements reveal that the multilayer HAPA films self-assemble in a reproducible manner with an index of refraction of 1.65 ± 0.04 at 632.8 nm , an interlayer spacing of $27 \pm 0.5 \text{ \AA/layer}$, and an average azobenzene chromophore tilt angle of $27 \pm 2^\circ$ from the surface normal. An electro-optic coefficient for the ultrathin HAPA multilayer films (r_{33}) of 11 pm/V at 632.8 nm was determined from electric field-modulated surface plasmon resonance measurements in air-gap capacitors. These preliminary results indicate that the self-assembly technique may serve as an alternative route to the formation of noncentrosymmetric thin films for electro-optical applications, as has been suggested by other researchers.^{21–24,60}

Noncentrosymmetric HAPA films were also shown to be valuable probes of the electrostatic fields in organic monolayers at electrochemical interfaces. A comparison of the in situ electro-optical response of ZP films at electrode surfaces with the results obtained from air-gap capacitors resulted in an in situ measurement of $1 \times 10^4 \text{ V/cm}$ for the electric field strength within the organic thin film. This field strength suggests that for this particular ZP film the electrolyte ions that form the electrochemical double layer at the interface do not penetrate into the organic film and reside primarily on the surface of the multilayer. Future experiments will focus on the systematic incorporation of HAPA chromophores into self-assembled multilayers in order to determine the electric field profile within various ultrathin organic films at electrochemical interfaces.

ACKNOWLEDGMENT

The authors gratefully acknowledge the support of the National Science Foundation in these studies. The authors also thank Dr. J. W. Taylor and his research group for the use of the ellipsometer in these studies.

Received for review July 26, 1996. Accepted August 1, 1996.[⊗]

AC960756+

[⊗] Abstract published in *Advance ACS Abstracts*, September 15, 1996.

- (66) Socrates, G. *Infrared Characteristic Group Frequencies*; Wiley: Chichester, England, 1980.
- (67) Lin-Vien, D.; et al. *The Handbook of Infrared and Raman Characteristic Frequencies of Organic Molecules*; Academic: Boston, 1991.
- (68) Thomas, L. C. *Interpretation of the Infrared Spectra of Organophosphorus Compounds*; Heyden: London, 1974.
- (69) Sverdlov, L. M.; Kovner, M. A.; Krainov, E. P. *Vibrational Spectra of Polyatomic Molecules*; Wiley: New York, 1974.
- (70) Bouquet, M.; Chassaing, G.; Corset, J.; Favrot, J.; Limouzi, J. *Spectrochim. Acta* **1981**, *37A*, 727.